Glycosylation-dependent galectin–receptor interactions promote *Chlamydia trachomatis* infection

Agustin L. Lujan[a,b], Diego O. Croci[c,d,1], Julián A. Gambarte Tudela[a,b,1], Antonella D. Losinno[a,b], Alejandro J. Cagnoni[e], Karina V. Mariño[e], María T. Damiani[a,b,2,3], and Gabriel A. Rabinovich[d,f,2,3]

[a]Laboratorio de Fagocitosis, Instituto de Histología y Embriología de Mendoza, Consejo Nacional de Investigaciones Científicas y Técnicas, Facultad de Ciencias Médicas, Universidad Nacional de Cuyo, C5500 Mendoza, Argentina; [b]Área de Química Biológica, Facultad de Ciencias Médicas, Universidad Nacional de Cuyo, C5500 Mendoza, Argentina; [c]Laboratorio de Inmunopatología, Instituto de Histología y Embriología de Mendoza, Consejo Nacional de Investigaciones Científicas y Técnicas, Facultad de Ciencias Exactas y Naturales, Universidad Nacional de Cuyo, C5500 Mendoza, Argentina; [d]Laboratorio de Inmunopatología, Instituto de Biología y Medicina Experimental, Consejo Nacional de Investigaciones Científicas y Técnicas, C1428ADN Buenos Aires, Argentina; [e]Laboratorio de Glicómica Funcional y Molecular, Instituto de Biología y Medicina Experimental, Consejo Nacional de Investigaciones Científicas y Técnicas, C1428ADN Buenos Aires, Argentina; and [f]Departamento de Química Biológica, Facultad de Ciencias Exactas y Naturales, Universidad de Buenos Aires, C1428EGA Buenos Aires, Argentina

Contributed by Gabriel A. Rabinovich, May 3, 2018 (sent for review February 6, 2018; reviewed by Sachiko Sato and Gerardo R. Vasta)

***Chlamydia trachomatis* (*Ct*) constitutes the most prevalent sexually transmitted bacterium worldwide. Chlamydial infections can lead to severe clinical sequelae including pelvic inflammatory disease, ectopic pregnancy, and tubal infertility. As an obligate intracellular pathogen, *Ct* has evolved multiple strategies to promote adhesion and invasion of host cells, including those involving both bacterial and host glycans. Here, we show that galectin-1 (Gal1), an endogenous lectin widely expressed in female and male genital tracts, promotes *Ct* infection. Through glycosylation-dependent mechanisms involving recognition of bacterial glycoproteins and *N*-glycosylated host cell receptors, Gal1 enhanced *Ct* attachment to cervical epithelial cells. Exposure to Gal1, mainly in its dimeric form, facilitated bacterial entry and increased the number of infected cells by favoring *Ct*–*Ct* and *Ct*–host cell interactions. These effects were substantiated in vivo in mice lacking Gal1 or complex β1–6-branched *N*-glycans. Thus, disrupting Gal1–*N*-glycan interactions may limit the severity of chlamydial infection by inhibiting bacterial invasion of host cells.**

sexually transmitted diseases | galectin-1 | glycosylation | host–pathogen interactions | *Chlamydia trachomatis*

The bacteria *Chlamydia trachomatis* (*Ct*) is the most common agent responsible of sexually transmitted diseases worldwide and the leading cause of infectious blindness in developing countries (1). This pathogenic microorganism causes a broad range of genitourinary diseases from mild acute infections to chronic disorders with deleterious consequences for human health and reproduction (2). As the majority of chlamydial genital infections in women are asymptomatic, they often remain untreated, leading to severe complications such as pelvic inflammatory disease, ectopic pregnancy, and tubal infertility (3). Additionally, *Ct* may be a risk factor for cervical cancer (4). Hence, chlamydial infections emerge as a public health concern of primary importance due to their high prevalence among young women and the lack of an effective preventive vaccine.

Ct is an obligate intracellular bacterium whose natural hosts are humans. *Ct* has a biphasic life cycle which alternates between two distinct developmental forms: (*i*) the elementary body (EB), a metabolically inert infectious form, and (*ii*) the reticulate body (RB), a metabolically active but noninfectious replicative form. After attachment and invasion of host epithelial cells, the EB rapidly undergoes a transformation to the RB, which multiplies by binary fission within the confines of a chlamydial-modified phagosome, termed the inclusion. An increase of RBs triggers differentiation back into EBs which are rapidly released to disseminate infection into neighboring cells (5). A successful intracellular infection relies on the ability of bacteria to manipulate the host cell molecular machinery to facilitate its entry and invasion, as well as its capacity to avoid lysosomal degradation and evade immune attack (5, 6). Given that the entire *Ct* life cycle occurs intracellularly, a critical event for establishing chlamydial infection is bacterial attachment, a two-step process involving early reversible interactions followed by a high-affinity irreversible association required for entry into host cells. Multiple bacterial ligands and host receptors have been implicated in *Ct* recognition and uptake (7), although the precise mechanisms underlying bacterial–host interactions are still uncertain.

Initial studies showed that the *Ct* major outer membrane protein (MOMP) binds to both mannose receptor and mannose 6-phosphate receptor, interactions that modulate infection in vitro (8). In addition, the chlamydial outer membrane complex protein B (OmcB) interacts with heparan sulfate proteoglycans (9–11). Moreover, both MOMP and OmcB bind to glycosaminoglycans, favoring synergistic electrostatic interactions required to initiate invasion (12, 13). Furthermore, several chlamydial

Significance

***Chlamydia trachomatis* (*Ct*) is the most common bacterium responsible for sexually transmitted infections. It constitutes a major public health burden, with the greatest clinical impact occurring in women of reproductive age. A vast proportion of *Ct* infections are underestimated because they are asymptomatic in nature. This leads to chronic infections with severe consequences, such as ectopic pregnancy, tubal obstruction, infertility, and blindness. *Ct* is an obligate intracellular pathogen that completes its entire developmental cycle in humans. Here, we demonstrate that galectin-1 (Gal1), an endogenous glycan-binding protein, promotes *Ct*–host adhesion and invasion. Through glycosylation-dependent mechanisms, Gal1 enhances chlamydial infection by favoring *Ct*–host cell interactions. Thus, novel therapeutic approaches aimed at disrupting Gal1–*N*-glycan interactions may reduce the severity of *Ct* infections.**

Author contributions: A.L.L., D.O.C., K.V.M., M.T.D., and G.A.R. designed research; A.L.L., D.O.C., J.A.G.T., A.D.L., and A.J.C. performed research; M.T.D. and G.A.R. contributed new reagents/analytic tools; A.L.L., D.O.C., J.A.G.T., A.D.L., A.J.C., K.V.M., M.T.D., and G.A.R. analyzed data; and A.L.L., K.V.M., M.T.D., and G.A.R. wrote the paper.

Reviewers: S.S., Laval University; and G.R.V., University of Maryland School of Medicine.

The authors declare no conflict of interest.

[1]D.O.C. and J.A.G.T. contributed equally to this work.

[2]M.T.D. and G.A.R. contributed equally to this work.

[3]To whom correspondence may be addressed. Email: meteresadamiani@gmail.com or gabyrabi@gmail.com.

This article contains supporting information online at www.pnas.org/lookup/suppl/doi:10.1073/pnas.1802188115/-/DCSupplemental.

ligands have been shown to interact with glycosylated epithelial receptors including β_1 integrin, EphrinA2 receptor, platelet-derived growth factor receptor (PDGFR)β, and fibroblast growth factor receptor (FGFR) (14–17). However, despite considerable progress, the endogenous mediators that link bacterial glycans and host receptors have not been identified.

Galectins, a family of endogenous glycan-binding proteins, play pivotal roles in inflammation, immunity, and cancer by modulating cell communication, signaling, adhesion, and migration (18–20). Emerging evidence suggests that galectins are also involved in host–microbial recognition and pathogen subversion of immune responses (21–25). Galectin-1 (Gal1), a 14.5-kDa member of this family, displays an evolutionary conserved carbohydrate-recognition domain (CRD) which can homodimerize. Gal1 recognizes multiple β-D-galactopyranosyl-(1–4)-*N*-acetyl-D-glucosamine (LacNAc) units, which are present on the branches of *N*- or *O*-linked glycans and are created by the concerted action of specific glycosyltransferases. This includes the *N*-acetylglucosaminyltransferase 5 (MGAT5), an enzyme that generates β1–6-*N*-acetylglucosamine (β1–6GlcNAc)-branched complex *N*-glycans, which are the preferred intermediates for LacNAc extension (19). This prototype lectin has been implicated in glycan-mediated recognition, invasion, and evasion by various pathogens including parasites like *Trypanosoma cruzi* and *Trichomonas vaginalis* (25–28) and viruses such as the human T-cell leukemia virus-1, HIV-1, influenza virus, dengue virus, Epstein–Barr virus, Nipah virus, and Enterovirus 71 (29–35).

With regards to bacterial infections, desialylation of airway epithelial cells by neuraminidases enhances adhesion of *Streptococcus pneumoniae* by facilitating Gal1 binding to specific glycans (36). Moreover, we recently found that the enteropathogenic bacterium *Yersinia enterocolitica* represses protective immune programs via Gal1-dependent pathways (37). Furthermore, in a model of *Pseudomonas aeruginosa* infection, Gal1 suppresses corneal immunopathology by limiting pathogenic Th17 responses (38). Interestingly, several pathogenic bacteria including *Helicobacter pylori* can themselves control genes involved in glycan biosynthesis, thus altering sensitivity to bacterial adhesins and endogenous lectins (39).

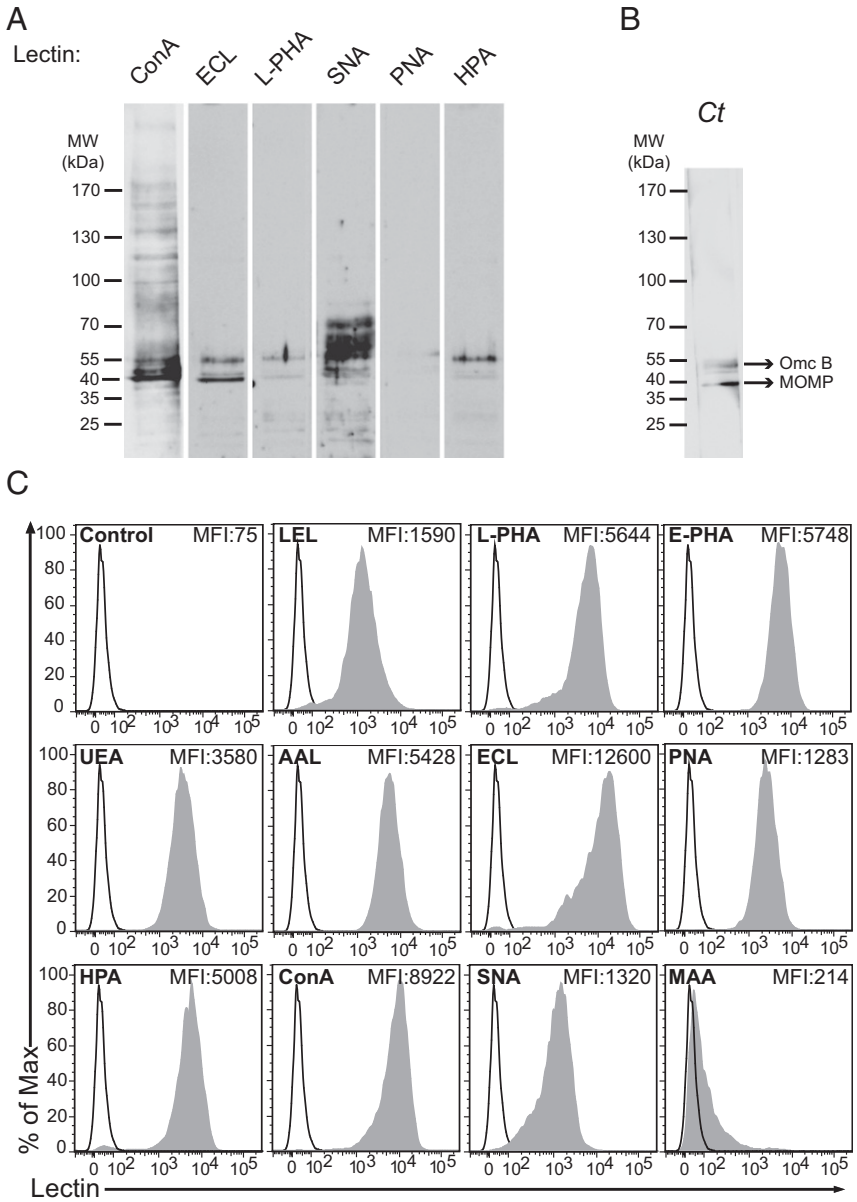

Fig. 1. Cell surface glycan profiles of *Ct* and HeLa cells. (*A*) Lectin blot analysis of whole-cell lysates of *Ct* infectious forms (EBs) detected with biotinylated lectins followed by streptavidin-HRP. (*B*) Western blot analysis of MOMP and OmcB expression in whole bacterial cell lysates. (*C*) Glycophenotype of HeLa cells detected with biotinylated lectins and PE-conjugated streptavidin (filled curve) or incubated with PE-conjugated streptavidin alone (control; empty curve) analyzed by flow cytometry. In *A* and *B* blots are representative of three independent experiments. In *C* histograms are representative of three independent experiments.

Here, we identified a central role for Gal1–*N*-glycan interactions in *Ct* recognition, attachment, and invasion of human cervical epithelial cells and have validated the relevance of these interactions in an experimental infection model in vivo. These findings set the basis for developing Gal1-targeted strategies to either prevent or attenuate chlamydial infection.

Results

Gal1 Binds to *Ct* and Host Cell Glycoproteins in a Glycan-Dependent Fashion. To explore the impact of Gal1–glycan interactions in *Ct* infection, we first assessed the glycophenotype of both the chlamydial cell wall and cervical epithelial host cells using a panel of biotinylated plant lectins. These proteins recognize specific glycan epitopes, including those that are relevant for Gal1 binding (*SI Appendix*, Table S1). Six lectins with different glycan affinities were individually tested against proteins of chlamydial EBs separated by SDS/PAGE (Fig. 1*A*). Lectin blotting revealed the presence of high-mannose structures, as indicated by Con A binding. Most intensely labeled are bands migrating at 40 and 55 kDa, which are molecular weights (MW) corresponding to MOMP and OmcB proteins (Fig. 1 *A* and *B*). Moreover, both the 40- and 55-kDa bands bound *Erythrina cristagalli* (ECL), a lectin capable of recognizing terminal *N*-acetyllactosamine (LacNAc) in non-α2–6-sialylated complex *N*-glycans and other glycoconjugates; only the 55-kDa band showed high reactivity for L-phytohemagglutinin (L-PHA), a lectin specific for β1–6-branched complex *N*-glycans. Notably, probing with *Sambucus nigra* agglutinin (SNA) demonstrated α2–6 sialylation in several chlamydial glycoproteins in the range of 55–70 kDa. Interestingly, no peanut agglutinin (PNA) reactivity was observed, suggesting that chlamydial glycoproteins may not be significantly enriched in asialo core-1 *O*-glycans (Fig. 1*A* and *SI Appendix*, Table S2). These results suggest that, in addition to well-known *N*-glycan high-mannose structures (40), a diverse repertoire of LacNAc-enriched glycoproteins is present in *Ct* which may serve as potential ligands for Gal1 binding. In this regard, α2–6 sialylation, a glycan modification that prevents Gal1 binding, was found in higher-MW glycoproteins (Fig. 1*A*), suggesting that Gal1 recognition may be limited to proteins in the low-MW range, such as MOMP and OmcB. Thus, *Ct* displays a broad glycosylation profile that could differentially control Gal1 binding.

To characterize the glycan signature of human cervical epithelial cells, we used HeLa cells as a model (41, 42). Cells were collected and incubated with different biotinylated lectins (*SI Appendix*, Table S1). Glycophenotypic analysis revealed high frequency of glycans permissive for Gal1 binding as shown by *Lycopersicon esculentum*- and ECL-reactive poly-LacNAc-enriched glycan epitopes and β1–6-branched complex *N*-glycans detected by L-PHA binding. Furthermore, we detected PNA-reactive asialo core-1 *O*-glycans on the surface of HeLa cells. Interestingly, α2–6-linked, but not α2–3-linked, sialic acid was preferentially detected on HeLa cells as shown by high SNA but undetectable *Maackia amurensis* agglutinin staining (Fig. 1*C*). A broader characterization of glycosylated ligands showed the presence of fucosylated structures on the surface of these cells as detected by the fucose-binding lectins *Ulex europaeus* agglutinin and *Aleuria aurantia* lectin, the presence of terminal GalNAc by *Helix pomatia* agglutinin binding, abundance of high-mannose structures determined by Con A, and extensive exposure of bisecting GlcNAc residues in *N*-glycans as evidenced by E-PHA recognition (Fig. 1*C*).

Furthermore, direct Gal1 binding to chlamydial glycoproteins was determined by separating EB proteins by SDS/PAGE and blotting with biotinylated Gal1. We confirmed reactivity of at least six chlamydial glycoproteins recognized by Gal1, including protein bands detected at 28, 37, 40, 42, 55, and 105 kDa (Fig. 2*A*). Moreover, Gal1 binding to HeLa cells was verified by lectin cytometry using biotinylated Gal1 as a probe (Fig. 2*B*). To further evaluate glycan-dependent binding of Gal1 to *Ct* cells, we incubated isolated EBs with recombinant Gal1, centrifuged and subsequently washed in the presence of lactose (100 mM) to displace Gal1 binding (*SI Appendix*, Fig. S1). Each subsequent pellet (EB+Gal1, EB1, and EB2) and eluted (E1) samples were lysed and separated by SDS/PAGE (Fig. 2*C*). MOMP and Gal1 were detected using specific polyclonal antibodies. Association of Gal1 with EBs was displaced by washing with lactose, suggesting carbohydrate-dependent binding of this lectin to the bacteria. Thus, Gal1 specifically associates with the surface of both *Ct* and human cervical epithelial cells through glycan-dependent mechanisms, suggesting a role for this lectin in modulating *Ct*–host cell interactions.

Chlamydial Infection Modulates Gal1 Expression and Subcellular Distribution in HeLa Cells. To understand the role of Gal1 during *Ct* infection, we investigated the regulated expression of this glycan-binding protein following exposure of HeLa cells to *Ct* EBs. Endogenous Gal1 was analyzed by Western blot in uninfected (control) and infected (*Ct*) host cells immediately after *Ct* binding [0 h postinfection (pi)] and 1 h pi. Exposure to *Ct* resulted in 40% increase in Gal1 protein content 1 h after chlamydial infection (Fig. 2*D*). Moreover, *Ct* infection altered subcellular distribution of Gal1 from a uniform cytosolic and membrane-associated pattern toward a membrane profile localized around the chlamydial inclusion area within the infected cells (Fig. 2*E*). This finding was confirmed by analysis of the distribution of endogenous Gal1 (green) and DAPI-labeled bacteria (blue) along a line traversing the chlamydial inclusion. Of note, whereas DAPI labels both eukaryotic and bacterial DNA, chlamydial inclusions (I) can be clearly distinguishable from nuclear (N) host DNA by means of intensity and compartmentalization. Intensity profile displayed two green peaks flanking the blue staining, indicating the presence of Gal1 at the boundaries of the inclusion area containing bacteria (Fig. 2*E*, *Middle* and *Right*). Furthermore, *xz* and *yz* projections confirmed Gal1 recruitment to the chlamydial inclusion area (Fig. 2*F*). This effect was further substantiated by analysis of *z*-sections using confocal microscopy, revealing significant association of Gal1 with chlamydial inclusions. The different optical planes revealed a fine punctuate pattern of endogenous Gal1 surrounding the inclusion with DAPI-labeled bacteria inside. Notably, Gal1 labeling was clearly detected within chlamydial inclusions (Movie S1). Thus, *Ct* infection modulates subcellular compartmentalization of Gal1, suggesting a potential role for this lectin in *Ct*–host cell interactions.

Gal1 Promotes *Ct* Attachment to Host Cervical Epithelial Cells. Chlamydial invasion of host cells initially requires bacterial recognition and adhesion to the target cell surface (5). To examine the impact of Gal1–glycan interactions on bacterial attachment to host cells, we first incubated HeLa cells with an increasing number of *Ct* (one or three bacteria per host cell) during the binding step at 4 °C and washed cells thoroughly. A higher number of adherent bacteria (evidenced by MOMP expression) was accompanied by higher levels of endogenous Gal1 in whole-cell lysates (Fig. 3*A*), suggesting a role for this lectin in modulating the attachment process. To assess this effect directly, we exposed HeLa cells to GFP-expressing *Ct* in the presence of increasing concentrations of recombinant Gal1 (ranging from 0.1 to 5 μM) at 4 °C; this allows bacteria to attach yet prevents their entry into host cells. Cells were washed extensively to remove unbound bacteria and Gal1 and further incubated for 24 h at 37 °C to allow bacterial internalization and development of chlamydial inclusions. The number of infected cells as well as the magnitude of intracellular bacterial load was analyzed by flow cytometry. Exposure to Gal1 significantly increased the percentage of infected cells in a dose-dependent manner, reaching a plateau at 1 μM (Fig. 3*B* and *SI Appendix*, Fig. S2*B*). Accordingly,

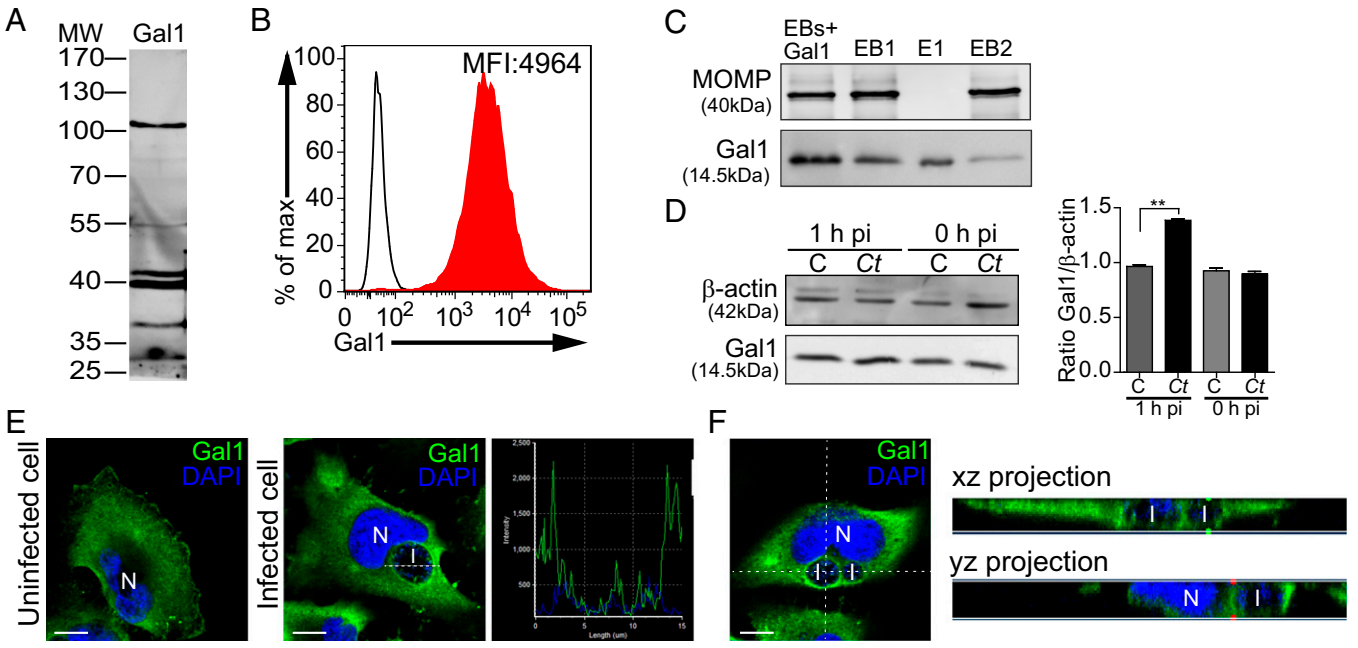

Fig. 2. Regulated expression, subcellular distribution, and binding of Gal1 to bacterial and host cell glycoproteins. (*A*) Binding of biotinylated Gal1 to *Ct* glycoproteins detected by lectin blotting. (*B*) Binding of biotinylated Gal1 to HeLa cells detected with PE-conjugated streptavidin (filled curve) and control cells incubated with PE-conjugated streptavidin alone (empty curve), assessed by flow cytometry. (*C*) Analysis of carbohydrate-dependent binding of Gal1 to EBs. Bacteria were incubated with 0.3 μM recombinant Gal1 (EB+Gal1) and washed twice with 100 mM lactose as indicated in *Materials and Methods*. Bacterial pellets (EB+Gal1, EB1, and EB2) and eluate (E1) were resolved by SDS/PAGE. MOMP and Gal1 were detected using specific polyclonal antibodies. (*D*) Immunoblot analysis of endogenous Gal1 in uninfected control (C) or infected (*Ct*) HeLa cells. β-actin was used as loading control (*Left*). Ratio of Gal1/β-actin expression in uninfected vs. infected cells (*Right*). (*E*) Confocal microscopy of subcellular Gal1 distribution upon infection. Uninfected HeLa cells (*Left*) and cells infected with *Ct* (MOI 1) for 18 h (*Middle*) are shown. (*Right*) The intensity profile scanned along a line crossing the inclusion area. (Scale bars, 10 μm.) (*F*) A single *xy* section from the stack of images of a HeLa cell infected for 18 h. *xz* and *yz* projections are shown aside the image. I, chlamydial inclusion; N, nucleus. Data are representative of three independent experiments. In *A*, *C*, and *D* blots are representative of at least three independent experiments. In *D* bars represent the mean ± SEM of three independent experiments (**$P < 0.01$).

a maximum in target cell infection was attained at 1 μM Gal1 concentration, indicating that bacterial internalization is a receptor-mediated process (Fig. 3*C*). Mean fluorescence intensity (MFI) correlated with the extent of fluorescently labeled bacteria distributed within each individual target cell. Interestingly, the number of bacteria per cell also increased following Gal1 exposure, likewise in a dose-dependent fashion until a plateau was reached at 0.3 μM (Fig. 3*D*). We conclude that extracellular Gal1 increases *Ct* adhesion and entry into HeLa cells in a dose-dependent manner.

Typically, Gal1 occurs in a monomer–dimer equilibrium that controls its biological activity. To investigate the contribution of Gal1 dimerization to bacteria–host cell interactions, we used a stable Gal1 variant (mGal1) generated by site-directed mutagenesis that maintains its carbohydrate-binding activity but cannot dimerize at the concentrations used (43). Addition of 1 μM mGal1 during bacterial attachment at 4 °C was substantially less efficient in increasing *Ct* adhesion and invasion of host cells compared with the WT lectin (Fig. 3*E*). Moreover, the number of fluorescent bacteria internalized per cell also dropped significantly when exposed to mGal1 compared with WT Gal1 (1 μM) (Fig. 3*F*). These results were further confirmed by confocal microscopy, which showed an increased frequency of infected cells and a greater number of chlamydial inclusions when bacteria were added to HeLa cells in the presence of WT but not mutant mGal1 (Fig. 3*G*). Fig. 3*G*, *Insets* show the size of chlamydial inclusions and the number of GFP-labeled bacteria. Thus, Gal1 dimerization optimizes chlamydial adhesion to host cells and likewise enhances bacterial infection.

Gal1 Facilitates Chlamydial Invasion of Host Cells. The ability of Gal1 to bind to both chlamydial and host glycans prompted us to analyze the contribution of this lectin to bacterial engulfment at the ultrastructural level. Briefly, HeLa cells were incubated with *Ct* in the absence or presence of 1 μM Gal1 at 4 °C (binding step), then cells were washed and maintained at 37 °C for different pi periods (15 min or 2 h). Thereafter, cells were fixed and processed for electron microscopy. Representative images are shown in Fig. 4*A*. The presence of WT Gal1 induced an increase in the number of chlamydial inclusions found in HeLa cells at 2 h pi (Fig. 4 *A* and *C*) compared with cells infected under control conditions (Fig. 4 *A* and *B*). However, addition of the mGal1 mutant during the binding step was much less efficient than the WT lectin in generating inclusion foci within infected cells (Fig. 4 *A* and *D*). Furthermore, we found a significant increase in inclusions containing two bacteria in cells incubated with WT Gal1 compared with those exposed to mGal1 or cultured in the absence of these lectins (Fig. 4*E*). To investigate this observation further, we analyzed cells at very early stages of infection and found nascent phagosomes including more than one *Ct* only when infection occurred in the presence of the WT lectin (Fig. 4*A*). Taken together, these findings suggest that Gal1 not only mediates bacterial adhesion to host glycans but may also promote *Ct* association, thus facilitating concomitant internalization of more than one bacteria.

These results are in agreement with the increased number of fluorescent bacteria per cell when cells were infected in the presence of WT Gal1 (Fig. 3*F*). Thus, Gal1, mainly in its dimeric form, facilitates bacterial internalization by engaging both chlamydial and host *N*-glycans.

Gal1 Enhances Chlamydial Adhesion to Host Cells Through Binding to *N*-Glycosylated Receptors. To provide additional confirmation regarding *N*-glycans and their role in mediating Gal1-induced *Ct*

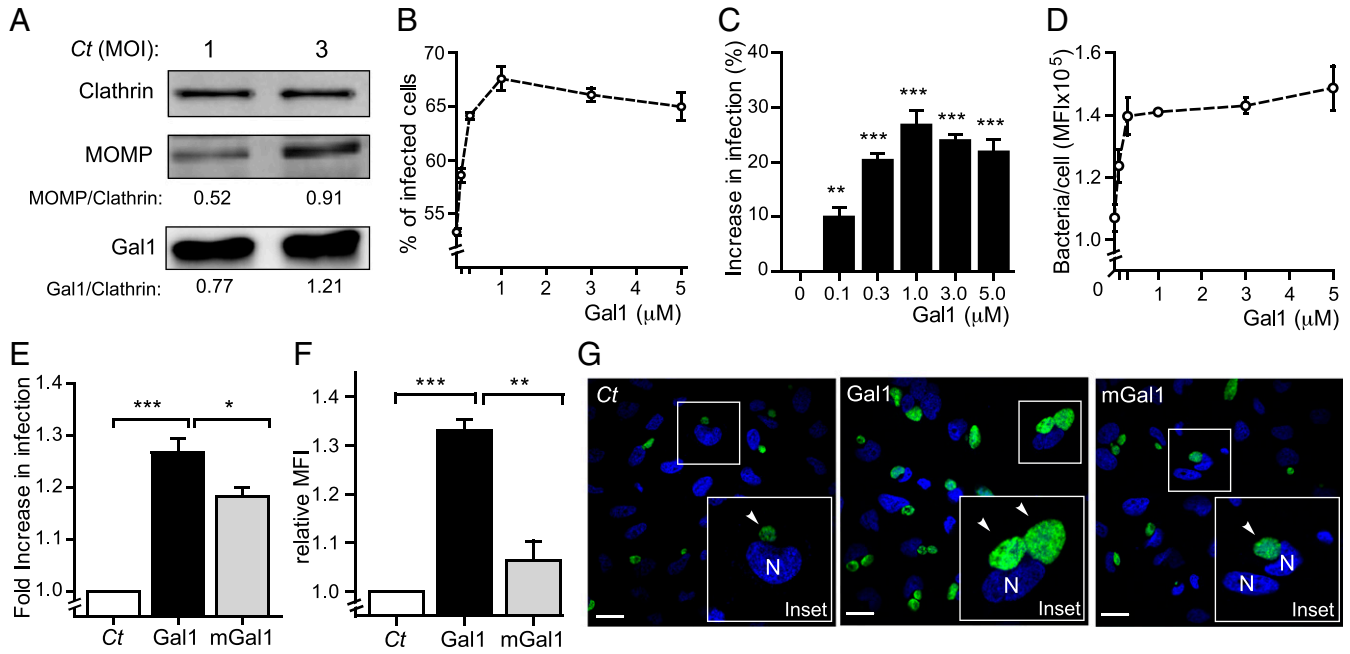

Fig. 3. Promotion of *Ct* adhesion and infection by Gal1. (*A*) Immunoblot analysis of endogenous Gal1 in HeLa cells incubated with different *Ct* numbers (MOI 1 and 3) during the binding step at 4 °C. Clathrin was used as loading control. (*B–D*) HeLa cells were infected with *Ct* (green) (MOI 0.5) in the presence of increasing concentrations of recombinant Gal1 (0.1–5 μM) during the binding step at 4 °C and analyzed by flow cytometry. (*B*) Percentage of infected HeLa cells at 24 h pi. (*C*) Fold increase in infection at 24 h pi. (*D*) Quantification of bacteria per cell measured by MFI at 24 h pi. (*E–G*) HeLa cells were infected with *Ct* (green) in the absence or presence of 1 μM WT Gal1 or mGal1 during the binding step at 4 °C. (*E*) Fold increase in infection at 24 h pi analyzed by flow cytometry. (*F*) Fold increase in the number of bacteria per cell determined by relative MFI at 24 h pi. In *C*, *E*, and *F* bars are the mean ± SEM (*$P < 0.05$, **$P < 0.01$, ***$P < 0.001$). (*G*) Representative micrographs of *Ct*-infected HeLa cells (green) by confocal microscopy. Arrowheads in insets indicate chlamydial inclusions. DNA was stained with DAPI (blue). (Scale bars, 10 μm.) N, nucleus. Data are representative of five independent experiments performed in triplicates, except in *A*, where experiments were performed twice.

attachment to host cells, we released complex *N*-glycans from the surface of uninfected HeLa cells by enzymatic cleavage with PNGase F. Flow cytometric analysis of L-PHA–stained cells confirmed a decrease in complex β1–6-branched *N*-glycans (Fig. 5*A*). Loss of host *N*-glycans led to a significant reduction in the number of *Ct*-infected HeLa cells (Fig. 5*B*), resulting in 50% reduction of chlamydial infectivity (Fig. 5*C*). As α2–6 sialylation of terminal LacNAc residues prevents Gal1 binding (44), we removed these moieties from cell surface glycoproteins of HeLa cells using neuraminidase A; loss of α2–6-linked sialic acid was confirmed by elimination of SNA labeling (Fig. 5*D*). Neuraminidase A treatment facilitated Gal1 binding and consequently enhanced chlamydial infection by ∼50% (Fig. 5 *E* and *F*). These results indicate that Gal1 modulates binding and entry of *Ct* into human cervical epithelial cells in an *N*-glycan–dependent fashion.

To explore further the mechanisms underlying Gal1-mediated bacterial–host interactions, we next analyzed several *N*-linked glycoproteins which have been proposed as candidate *Ct* receptors (*SI Appendix*, Table S3) (45–48). We found substantial colocalization of Gal1 and *Ct* antigens with both PDGFRβ and $\beta_1/\alpha_V\beta_3$ integrins when HeLa cells were exposed to the bacteria; however, no significant overlapping could be detected among *Ct,* Gal1, and FGFR2 (Fig. 5*G*). To assess the functional contribution of these receptors to Gal1-mediated chlamydial invasion, we performed adhesion experiments in the absence or presence of specific neutralizing antibodies. The number of green fluorescent bacteria internalized per cell was measured by flow cytometry at 24 h pi. In agreement with the results of confocal microscopy, blocking PDGFRβ or $\beta_1/\alpha_V\beta_3$ integrins, but not FGFR2, significantly reduced the extent of bacterial infection promoted by Gal1 (Fig. 5*H*). This inhibitory effect was less pronounced when experiments were performed in the absence of exogenous Gal1 (*SI Appendix*, Fig. S2*A*). Thus, Gal1 promotes *Ct* invasion of host cervical cells, at least in part, through *N*-glycosylation–dependent interactions involving PDGFRβ and/or $\beta_1/\alpha_V\beta_3$ integrins.

Gal1–*N*-Glycan Interactions Favor *Ct* Infection in Vitro and in Vivo. To determine whether Gal1-mediated cross-linking of bacterial and host *N*-glycans could enhance the extent of chlamydial infection, we infected HeLa cells with green fluorescent *Ct* in the absence or presence of Gal1 or its monomeric mutant mGal1. After 48 h, internalized bacteria completed their developmental life cycle, then chlamydial progeny was collected and its ability to infect new cells was evaluated by confocal microscopy (Fig. 6*A*) and flow cytometry (Fig. 6*B*). As shown by inclusion-forming units assays, addition of WT Gal1 but not mGal1 generated a twofold increase in the yield of infectious EBs (Fig. 6 *A* and *B*).

To evaluate the contribution of Gal1 to chlamydial infection in vivo, we compared *Ct* infection of WT female mice in the presence or absence of recombinant Gal1 in an animal model of genital infection. Briefly, female C57BL/6 mice were intravaginally inoculated with green fluorescent *Ct*. At 14 d postinoculation (dpi), vaginal discharge was collected from each mouse with disposable microbrushes and used to infect cell cultures to assess the presence of chlamydial organisms. The yield of infectious particles released from each infected mouse correlated with the number and size of chlamydial inclusions generated in HeLa cell monolayers as determined by confocal microscopy (Fig. 6*C*). The number of fluorescent bacteria per cell, indicated by MFI, was assessed by flow cytometry (Fig. 6*C*, *Insets*). The addition of Gal1 during *Ct* challenge in vivo significantly increased genital infection compared with WT mice infected in the absence of the exogenous lectin. In agreement, the number of bacteria per cell, indicated by MFI, significantly augmented when vaginal discharges from mice infected in

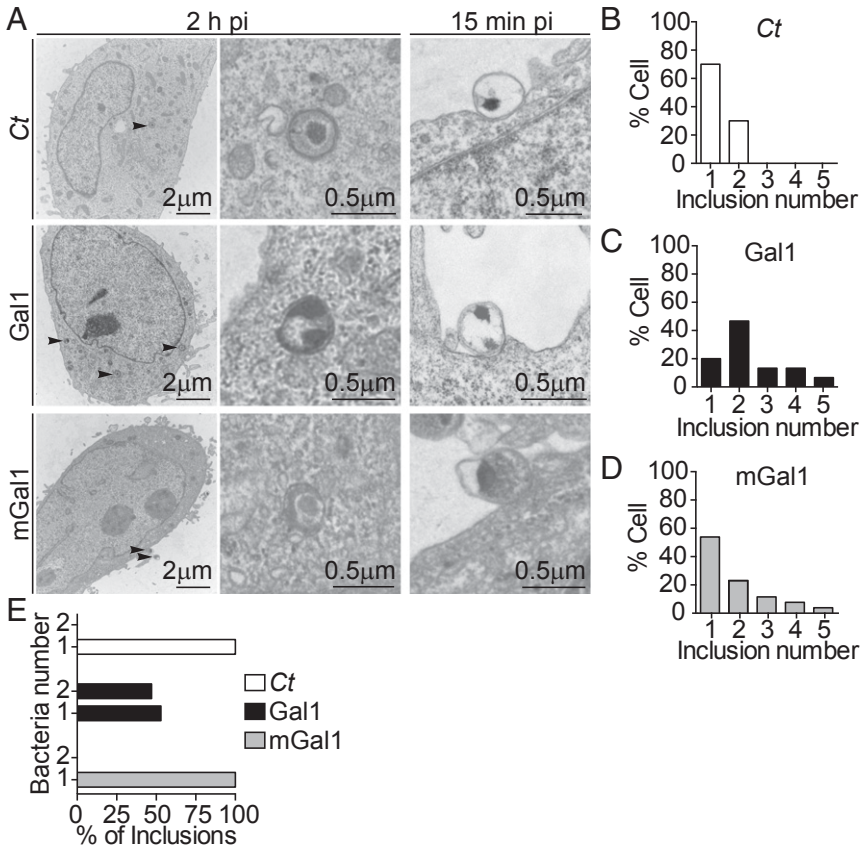

Fig. 4. Ultrastructural analysis of *Ct*-infected HeLa cells in the presence or absence of Gal1. (*A*) HeLa cells were infected with *Ct* (MOI 1) in the absence or presence of 1 μM Gal1 or mGal1 during the binding step at 4 °C. Cells were fixed at 15 min pi (*Right*) or 2 h pi (*Left* and *Middle*) and processed for transmission electron microscopy. Arrowheads show chlamydial inclusions. (*Middle* and *Right*) Magnifications of chlamydial inclusions. (*B–D*) Percentage of HeLa cells containing one or two *Ct* inclusions when incubated in the absence (*B*) or in the presence of 1 μM Gal1 (*C*) or mGal1 (*D*) during the binding step at 4 °C. (*E*) Percentage of *Ct* inclusions containing one or two bacteria in cells infected in the absence or in the presence of 1 μM Gal1 or mGal1 during the binding step at 4 °C. Data are representative of two independent experiments performed in duplicates.

the presence of exogenous Gal1 were assayed (Fig. 6*C*, *Ct* vs. Gal1).

Given the modulatory effects of exogenous Gal1, we then examined expression of this lectin in uteri from uninfected and *Ct*-infected mice. Immunohistochemical analysis of uterine tissue revealed significant up-regulation of Gal1 expression in response to chlamydial infection (Fig. 6*D*). This effect was accompanied by redistribution of this lectin, which shifted from a diffuse stromal localization in uninfected mice toward a focalized compartmentalization in simple columnar epithelium of *Ct*-infected mice (Fig. 6*D*). These results are in agreement with those observed in HeLa cells early after *Ct* infection (Fig. 2*D*).

To evaluate the impact of endogenous Gal1 and complex β1–6-branched *N*-glycans during chlamydial infection, similar experiments were performed in female mice lacking Gal1 ($Lgals1^{-/-}$) or MGAT5 ($Mgat5^{-/-}$). Although vaginal discharges obtained early after infection from $Lgals1^{-/-}$ and WT mice both generated a low number of inclusions in HeLa cells ex vivo (Fig. 6*C*, *Ct* vs. $Lgals1^{-/-}$ mice), immunoblot analysis of MOMP expression in whole uteri homogenates revealed a significant lower degree of *Ct* infection in $Lgals1^{-/-}$ vs. WT mice (Fig. 6*E*). Finally, vaginal discharges collected from $Mgat5^{-/-}$ mice displayed a considerably lower number of infectious *Ct* compared with WT mice (Fig. 6*C*, *Ct* vs. $Mgat5^{-/-}$). These findings were reinforced by immunoblot analysis of MOMP expression in uterine tissue from $Mgat5^{-/-}$ vs. WT infected hosts (Fig. 6*E*). Altogether, these results demonstrate the contribution of Gal1 as well as β1–6-branched complex *N*-glycans to the pathophysiology of chlamydial infection in vivo.

Discussion

Chlamydia is an obligate intracellular bacterium that must bind to epithelial host cells to initiate and establish infection (2). Host invasion may involve bacterial adhesins recognizing host carbohydrate moieties and host lectins interacting with bacterial glycoconjugates. Notably, chlamydial infectious forms (EBs) exhibit diversity in their adhesion profiles, as demonstrated by glycan arrays, capable of discriminating different *Chlamydia* species or serovars (7, 49). In this regard, previous studies reported the characterization of *N*-glycosylated proteins on the surface of *Ct* (8, 40, 50), which play essential roles in the process of infection. Inhibition of *N*-glycosylation with tunicamycin or specific cleavage of bacterial *N*-glycans decreased chlamydial infectivity (51). However, these studies have focused primarily on the role of high-mannose *N*-glycans and their interaction with host mannose-binding proteins (40, 51). Here we demonstrated that chlamydial membrane proteins of the infectious bacteria, particularly those exhibiting low MW, display a distinctive glycosylation pattern that is permissive for Gal1 binding.

Within the innate immune compartment, galectins are capable of functioning as pattern recognition receptors that bind to bacterial antigens and trigger complement activation, phagocytosis, and adaptive immunity (20, 21). Here we show that Gal1 binds to at least six chlamydial glycoproteins (gp28, gp37, gp40, gp42, gp55, and gp105) and interacts with certain host glycosylated receptors with permissive glycan structures for Gal1 recognition, such as PDGFRβ and $\beta_1/\alpha_V\beta_3$ integrins, suggesting a novel role for this endogenous lectin in facilitating *Ct* infection by bridging bacterial and host cell surface glycans. Although we examined the involvement of well-established glycosylated receptors in *Ct* invasion, our study does not exclude the possibility that other cell surface glycoproteins may contribute to this effect.

Given the bidirectional interaction of Gal1 with both chlamydial and host glycoproteins, we questioned whether this lectin could act at the bacterial–host cell interface either by promoting

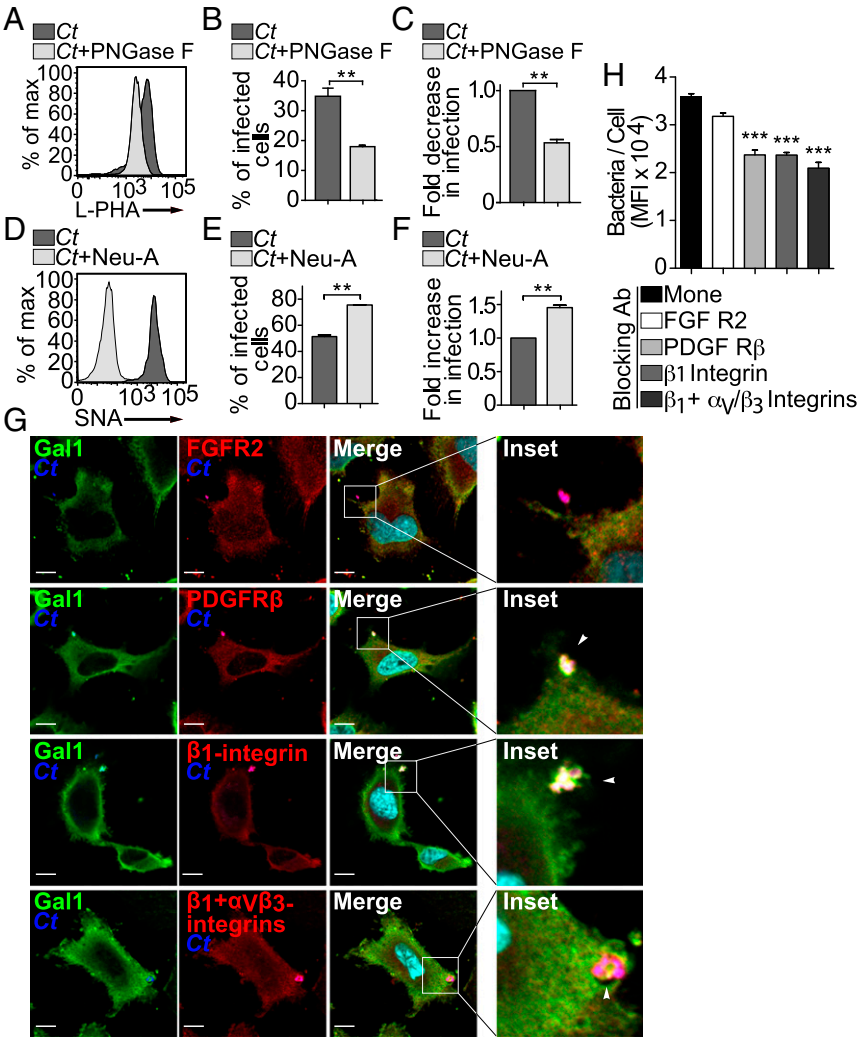

Fig. 5. Glycosylation-dependent *Ct* binding to host cell receptors promotes infection. (*A*–*C*) HeLa cells were pretreated with PNGase F to release *N*-glycans. (*A*) Analysis of L-PHA binding to untreated or PNGase F-treated cells by flow cytometry. (*B*) Percentage of infected HeLa cells determined by flow cytometry. (*C*) Fold decrease of *Ct* infection in PNGase F-treated cells. (*D*–*F*) HeLa cells were treated with neuraminidase A (Neu A) to release sialic acid. (*D*) Analysis of SNA binding to untreated and Neu A-treated cells by flow cytometry. (*E*) Percentage of infected HeLa cells by flow cytometry. (*F*) Fold increase of *Ct* infection in Neu A-treated cells. (*G*) Immunofluorescence detection of *N*-glycosylated receptors on HeLa cells incubated with *Ct* during the binding step at 4 °C (MOI 3). Infection was confirmed using an anti-MOMP antibody (blue). FGFR2, PDGFRβ, β_1-integrin, and $\alpha_V\beta_3$ integrins were detected using specific antibodies (red). Gal1 was detected using a rabbit anti-human Gal1 antibody (green). Arrowheads indicate triple colocalization. (Scale bars, 10 μm.) (*H*) Contribution of glycosylated receptors to Gal1-induced *Ct* infection. Quantification of bacteria per cell measured by MFI at 24 h pi in HeLa cells incubated with 1 μM recombinant Gal1 in the absence or presence of different neutralizing monoclonal antibodies. In *B*, *C*, *E*, *F*, and *H* data are the mean ± SEM of three experiments (**$P < 0.01$, ***$P < 0.001$). In *A*, *D*, and *G* data are representative of three independent experiments performed in triplicates.

or inhibiting chlamydial adhesion and invasion. Our results showed that incorporation of Gal1 during the recognition process enhances chlamydial attachment to epithelial cells in a dose-dependent manner, resulting in higher rates of infection. Notably, the number of infected cells reached a plateau, consistent with chlamydial internalization as a receptor-mediated process. Accordingly, Gal1 colocalized with PDGFRβ and $\beta_1/\alpha_V\beta_3$ integrins but not with FGFR2 at the bacterial–host cell boundaries and blockade of these receptors attenuated the extent of infection. In this regard, PDGFRβ blockade reduced binding of *Ct* to target cells (16). Moreover, the *Ct* invasin Ctad1 associated with β_1 integrins to invade host cells (14). Thus, Gal1 may serve as a bridge that connects glycosylated ligands present in both bacteria and host cell receptors including PDGFRβ and $\beta_1/\alpha_V\beta_3$ integrins. Whereas FGFR2 has been reported to be a potential receptor for *Chlamydia* infection (17), we could find no significant contribution of this growth factor receptor to Gal1-mediated effects; these results could be due, at least in part, to the nonpermissive glycosylation pattern of this particular receptor (45).

From a biochemical standpoint, Gal1 can form homodimers, acquiring bivalent carbohydrate-binding capacity which enables simultaneous cross-linking of glycosylated cell surface receptors (19). Our findings indicate that Gal1 dimerization is critical to promote optimal bacterial adhesion to target cells as the number of bacteria internalized per cell increased considerably with the addition of WT Gal1. Interestingly, although with much lower potency, mGal1 also promoted *Ct* attachment to target cells, suggesting the possibility that this monomeric mutant could influence dimer formation and/or cross-linking activity of the endogenous lectin. Furthermore, it is possible to speculate that Gal1 not only mediates chlamydial binding to host cells but also induces bacterial clustering. In fact, Gal1 enhanced adhesion of grouped *Ct* to host cells and increased the number of bacteria internalized per cell, as shown by electron microscopy. Supporting these findings, it has been demonstrated that Gal1 not only binds to cervical epithelial cells but also agglutinates *T. vaginalis* (26). The relevance of glycosylation in chlamydial attachment and infection induced by Gal1 was confirmed by elimination of *N*-glycans and desilalylation via enzymatic cleavage.

Since bacterial attachment to host cells is crucial for establishing chlamydial infection, we analyzed the impact of Gal1 on the generation of bacterial progeny. Addition of Gal1 during *Ct* binding resulted in a twofold increase in the yield of infectious bacteria by enhancing chlamydial adhesion to and invasion of HeLa cells. Although recombinant Gal1 was removed from extracellular media upon binding, an additional effect of Gal1 on chlamydial replication could not be ruled out and warrants further investigation. In agreement, intravaginal inoculation of mice in the presence of recombinant Gal1 enhanced chlamydial infection in vivo, as demonstrated by higher release of infectious bacteria in the vaginal discharge and increased MOMP expression in uterine tissue. Interestingly, *Ct* induced considerable up-regulation

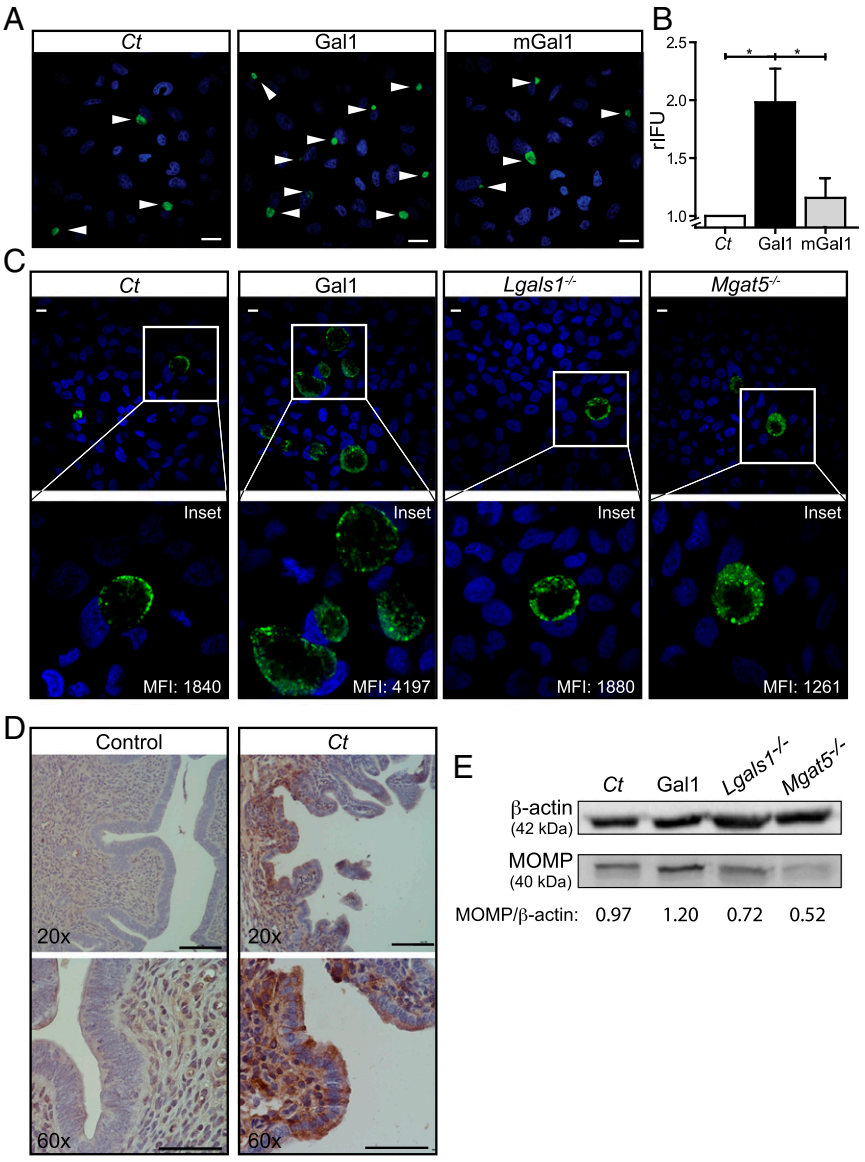

Fig. 6. Gal1 promotes chlamydial infection in vitro and in vivo. (*A* and *B*) HeLa cells were infected with *Ct* (green) (MOI 0.5) in the absence or presence of 1 μM recombinant Gal1 or mGal1. At the end of chlamydial developmental cycle (48 h pi), infected cells were lysed and the infectious particles were titrated in serial dilutions on HeLa cell monolayers. (*A*) Confocal microscopy of inclusions generated by progenies collected from chlamydial control (*Ct*), Gal1-treated, and mGal1-treated HeLa cells. Representative images show the inclusions (green) developed at 24 h pi. DNA was stained with DAPI (blue). Arrowheads indicate chlamydial inclusions. (Scale bars, 10 μm.) (*B*) Number of relative IFU (rIFU) generated by chlamydial progenies determined by flow cytometry (*$P < 0.05$). (*C* and *D*) Development of *Ct* infection in vivo. Female C57BL/6 mice were intravaginally infected with fluorescent *Ct* in the absence (*Ct*; $n = 10$) or presence of 1 μM recombinant Gal1 (Gal1; $n = 10$). Mice lacking Gal1 (*Lgals1*$^{-/-}$; $n = 10$) or MGAT5 (*Mgat5*$^{-/-}$; $n = 5$) were infected with *Ct*. At 14 dpi vaginal discharges were collected. (*C*) Confocal microscopy of inclusions (green) generated in HeLa cell monolayers exposed for 24 h pi to mice vaginal discharges. (*Insets*) Magnifications of the selected areas. MFI represents fluorescent intensity of bacterial inclusion determined by flow cytometry. (Scale bars, 10 μm.) (*D*) Immunohistochemical analysis of Gal1 expression in uteri sections from uninfected and *Ct*-infected mice. (Scale bars, 50 μm.) (*E*) Immunoblot analysis of bacterial MOMP in uterine tissue from chlamydial control (*Ct*), Gal1-treated, *Lgals1*$^{-/-}$, or *Mgat5*$^{-/-}$ mice. β-actin was used as loading control. Data are the mean ± SEM (*B*) or are representative (*A* and *C*–*E*) of three independent experiments.

of endogenous Gal1 both in vitro and in vivo, supporting a critical role for this lectin in modulating infection. Accordingly, uterine tissue from Gal1-deficient mice presented lower bacterial load as demonstrated by diminished levels of MOMP expression, although these differences could not be verified in vaginal discharges, probably due to the low sensitivity of this assay. Moreover, *Mgat5*$^{-/-}$ mice generated fewer infectious progeny, thus confirming the role of complex β1–6 branched *N*-glycans in chlamydial infection outcome. As several galectin family members may recognize LacNAc-enriched complex branched *N*-glycans (19), these findings may reflect the contribution of other galectins to *Ct*–host cell interactions.

Interestingly, we detected an initial increase of Gal1 expression in *Ct*-infected cells and striking changes in subcellular distribution of this lectin shifting from a broad cytosolic and membrane-associated pattern toward the formation of chlamydial inclusions in vitro. Furthermore, *Ct* infection in vivo led to changes in Gal1 distribution which turned from a stromal localization toward a columnar epithelial compartmentalization in uterine tissue. Likewise, Gal1 was found to be up-regulated and relocalized in response to infection with different types of bacteria, viruses, and parasites (21, 52).

Although a role of Gal1 in inducing attachment of viruses and parasites to human cells has been reported, there is still scarce information on the contribution of Gal1 to bacterial infections. Previous reports showed that Gal1 promotes binding of viral envelope gp120 to CD4$^+$ T cells, facilitating HIV-1 infection in a β-galactoside–dependent manner (30). Also, Gal1 promotes enterovirus 71 replication and enhances its infectivity (34). In contrast, Gal1 binding to *N*-linked oligosaccharides of hemagglutinin and neuraminidase from influenza virus masks relevant glycan structures and inhibits viral infection (31). Similarly, Gal1 inhibits dengue virus adsorption and internalization into target cells (32). However, Gal1 favors Nipah virus attachment to endothelial cells but inhibits the fusion of its envelope glycoproteins with target cells (33). Additionally, interactions between *T. vaginalis* lipophosphoglycan and Gal1 have been reported to control parasite infection of human cervical epithelial cells (26). Furthermore, low concentrations of Gal1 enhanced *T. cruzi* replication, whereas higher levels of this lectin inhibited this process (27, 28, 53). Regarding bacterial infections, Gal4 and Gal8, two-CRD galectins, have been shown to recognize and kill bacteria-expressing B– blood group antigens on their surface (54). Finally, pathogenic bacteria may also subvert recognition of host galectins

to ensure successful attachment and invasion of target cells leading to alteration of immune responses (37).

In conclusion, our study utilizes both in vitro and in vivo strategies to demonstrate that Gal1 favors the development of productive chlamydial infections by modulating attachment and internalization of bacteria into host cells via an *N*-glycan–dependent mechanism. In support of our findings, other sexually transmitted pathogens, including HIV-1 and *T. vaginalis*, exploit Gal1 as a critical mediator responsible of promoting infection (26, 30). As preexisting sexually transmitted diseases are significant risk factors for other sexually transmitted pathogens (including HIV-1), further studies should explore the relevance of Gal1 as a critical endogenous factor mediating coinfection. Thus, Gal1-specific antagonists (55) could be useful as a means to undermine chlamydial infection as well as other STDs. Understanding the role of galectin–glycan interactions at the pathogen–host cell interface may lead to development of novel therapeutic approaches aimed at attenuating bacterial infections.

Materials and Methods

Cell Culture, Antibodies, Recombinant Galectins, and Reagents. HeLa 229 cells were cultured in high glucose Dulbecco's modified Eagle's medium (Gibco BRL) supplemented with 10% (vol/vol) FBS (Internegocios SA), 0.3 mg/mL L-glutamine (ICN Biomedicals Inc.), and 1.55 mg/mL glucose (Biopack) without antibiotics in 5% CO_2 at 37 °C. Primary, neutralizing, and secondary antibodies used for blocking and labeling are listed in *SI Appendix*, Table S3. Recombinant Gal1 and the mGal1 variant were produced and purified as described (56, 57). Lipopolysaccharide content of the purified samples (<60 ng/mg) was tested using a Gel Clot Limulus Test (Cape Cod).

Bacterial Strains. *Ct* serovar L2 and *Ct*-transformed strain harboring p2TK2-SW2 IncD Prom-RSGFP-IncDTerm (GFP-overexpressing *Ct* L2) were generated and kindly provided by H. Agaisse and I. Derré, Yale University School of Medicine, New Haven, CT (58). Bacterial propagation was performed as described in *SI Appendix*. Aliquots were stored at −80 °C and thawed immediately before use.

Glycophenotype Analysis. HeLa cells were incubated with biotinylated lectins listed in *SI Appendix*, Table S1 as described (44). Flow cytometry analysis was performed using a BD FACSAria III (Becton Dickinson Biosciences). A minimum of 10,000 gated events were collected for each sample. Data were analyzed using FlowJo software.

For lectin blotting, 1×10^6 *Ct* were lysed (50 mM Tris, 150 mM NaCl, 10 mM EDTA, and 1% Nonidet P-40), solved in 10% SDS/PAGE, and transferred onto a 0.45-μm nitrocellulose membranes (GE Healthcare Life Science). Strips were probed with different biotinylated lectins as indicated (44). Immunoreactivity was visualized using horseradish rabbit peroxidase (HRP)-conjugated streptavidin (Sigma) and Pierce ECL Western blotting substrate (Thermo Fisher Scientific Inc) with an ImageQuant LAS 4000 (GE Healthcare Life Science).

Gal1 Binding and Deglycosylation Assays. Carbohydrate-dependent *Ct* binding assays were performed as described in *SI Appendix* (*SI Appendix*, Fig. S1). All bacterial pellets (EB, EB1, and EB2) and eluate (E1) were resolved on a 15% SDS/PAGE, transferred onto 0.45-μm nitrocellulose membranes (GE Healthcare), and incubated overnight with anti-Gal1 (1:1,000) or anti-MOMP (1:500) antibodies followed by goat anti-rabbit HRP-conjugated IgG (1:5,000, 1 h, 37 °C). Protein bands were visualized using Pierce ECL Western blotting substrate in an ImageQuant LAS 4000.

To examine the role of glycans in Gal1 effects, HeLa cells (1×10^5) were incubated with PNGase F (50 U, 37 °C, 4 h), α2–3/6/8/9 neuraminidase A (20 U, 37 °C, 1 h) (New England Biolabs), or 30 mM lactose (Sigma) before infection with fluorescent *Ct*. At 24 h pi, cells were gently detached using trypsin and stained with 30 μL propidium iodide (1:1,000). Cells were analyzed by flow cytometry.

***Ct* Binding to Host Cells and Receptor Neutralization Assays.** HeLa cells (1×10^5 cells/well) were preincubated in the absence or presence of recombinant Gal1 or its stable monomeric mutant mGal1 at different concentrations (0.1–5 μM) at 4 °C before addition of green fluorescent *Ct* [multiplicity of infection (MOI) 0.5]. Then, *Ct* was added to plates which were centrifuged at 400 × *g* for 15 min at 4 °C (binding step). Then, cells were washed three times with 500 μL cold PBS to remove unbound bacteria and the excess of Gal1. Finally, cells were incubated for 24 h in 5% CO_2 at 37 °C (infection period) and analyzed by flow cytometry as indicated above.

To study the involvement of *N*-glycosylated receptors, HeLa cells were incubated 30 min at 37 °C in the absence or presence of recombinant Gal1 and neutralizing antibodies to FGFR2 (0.5 μg/mL), PDGFRβ (20 μg/mL), β_1 integrin (10 μg/mL), and $\beta_1/\alpha_V\beta_3$ integrins (10 μg/mL) before infection with fluorescent *Ct*. Then, cells were analyzed by flow cytometry at 24 h pi to determine the amount of bacteria within each cell.

Immunoblotting. Immunoblot analysis was performed essentially as described (44). Briefly, equal amounts of protein were resolved by SDS/PAGE, transferred onto 0.45-μm nitrocellulose membranes, and incubated overnight with anti-MOMP (1:500), anti-Gal1 (1:1,000) and anti–β-actin (1:1,000) antibodies followed by goat anti-rabbit HRP-conjugated IgG (1:5,000, 1 h, 37 °C). Bands were visualized using Pierce ECL Western blotting substrate in an ImageQuant LAS 4000.

Immunofluorescence and Immunohistochemistry. HeLa cells (1×10^5 cells per well) grown on coverslips were infected with *Ct* for different time periods. To identify endogenous proteins, cells were fixed with 3% paraformaldehyde, quenched, and incubated with the appropriate primary antibodies followed by fluorescently labeled secondary IgG. Coverslips were mounted in Mowiol 4-88 with 0.5 μg/mL DAPI for DNA staining. Samples were observed under an Olympus FluoView FV1000 confocal microscope equipped with multiple filter sets. Images were processed using ImageJ software. For immunoperoxidase, paraffin-embedded uterine tissue sections were stained with rabbit anti-Gal1 IgG as described (59) using the Vectastain Elite ABC kit (Vector).

Transmission Electron Microscopy. HeLa cells were grown in T-25 flasks, infected with *Ct* (MOI 5), and fixed at 15 min or 2 h pi with 2.5% glutaraldehyde in 0.1 M sodium cacodylate buffer and processed as described in *SI Appendix*. Grids were examined with a Zeiss 900 electron microscope (Zeiss).

IFU Assay. To evaluate the effects of Gal1 on chlamydial replication, HeLa cells were preincubated with or without 1 μM recombinant Gal1 or mGal1 at 4 °C before addition of fluorescent *Ct* (MOI 0.5) and processed as described in *SI Appendix*.

Chlamydial Genital Infection in Mice. Six-week-old C57BL/6 female mice were bred and maintained under specific pathogen-free conditions. Animal protocols were approved by the Committee of Animal Care and Use Guidelines of the Faculty of Medicine, National University of Cuyo (CICUAL, FCM, UNCuyo). *Lgals1*$^{-/-}$ mice were provided by F. Poirier, Jacques Monod Institute, Paris, and *Mgat5*$^{-/-}$ mice were obtained from Jackson's Laboratories. To synchronize the murine estrous cycle, a single dose of 2.5 mg medroxyprogesterone acetate (Holliday Scott SA) was s.c. injected in each mouse 7 d before inoculation with *Ct*. Mice were divided into four groups: (*i*) *Ct* ($n = 10$) inoculated in WT mice; (*ii*) *Ct* inoculated in WT mice in the presence of 1 μM recombinant Gal1 (*Ct* + Gal1; $n = 10$); (*iii*) *Ct* inoculated in *Lgals1*$^{-/-}$ mice ($n = 10$); and (*iv*) *Ct* inoculated in *Mgat5*$^{-/-}$ mice ($n = 5$). Animals were inoculated intravaginally with 1.5×10^5 EBs under ketamine (Holliday Scott SA) and xylazine (König SA) anesthesia.

Analysis of Chlamydial Progenies Released in Vaginal Discharges. Vaginal discharges were collected with disposable microapplicators (Multi-Brush; Denbur Inc.) at 14 dpi and used for infecting HeLa cell monolayers grown on coverslips in 24-well plates for 48 h in the presence of gentamicin 50 μg/mL and processed as described in *SI Appendix*. Determinations were performed in three independent experiments in triplicates. Vaginal discharges were collected from two independent genital infection assays.

Statistical Analysis. Statistical analysis was performed using GraphPad Prism 5.0 Software (GraphPad). Data represent the mean ± SDs of *N* experiments. For simple unpaired analysis between two groups, Student's *t* test was chosen. For multiple comparisons, ANOVA with subsequent Bonferroni's or Dunnet's posttests was used. *P* values less than 0.05 were considered statistically significant.

ACKNOWLEDGMENTS. We thank R. Morales, S. Gatto, A. Fernández, and J. Scelta for dedicated animal care; A. Lafalla for advice with flow cytometry analysis; the staff of the Microscopy Platform for invaluable technical help; and Dr. Helene Rosenberg for critical reading of the manuscript. This work was supported by National Argentinean Agency for Promotion of Science and Technology Grants PICT 2012-2116 (to M.T.D.) and PICT 2012-2440 (to G.A.R.), Universidad Nacional de Cuyo Grant SECTyP 2016 (to M.T.D.), and Fundaciones Sales and Bunge & Born (G.A.R.).

1. World Health Organization (2011) Prevalence and incidence of selected sexually transmitted infections, *Chlamydia trachomatis*, *Neisseria gonorrhoeae*, syphilis and *Trichomonas vaginalis*: Methods and results used by WHO to generate 2005 estimate (WHO, Geneva), pp 1–38.
2. Elwell C, Mirrashidi K, Engel J (2016) *Chlamydia* cell biology and pathogenesis. *Nat Rev Microbiol* 14:385–400.
3. Menon S, et al. (2015) Human and pathogen factors associated with *Chlamydia trachomatis*-related infertility in women. *Clin Microbiol Rev* 28:969–985.
4. Zhu H, Shen Z, Luo H, Zhang W, Zhu X (2016) *Chlamydia trachomatis* infection-associated risk of cervical cancer: A meta-analysis. *Medicine (Baltimore)* 95:e3077.
5. Bastidas RJ, Elwell CA, Engel JN, Valdivia RH (2013) Chlamydial intracellular survival strategies. *Cold Spring Harb Perspect Med* 3:a010256.
6. Damiani MT, Gambarte Tudela J, Capmany A (2014) Targeting eukaryotic Rab proteins: A smart strategy for chlamydial survival and replication. *Cell Microbiol* 16: 1329–1338.
7. Cossé MM, Hayward RD, Subtil A (May 20, 2016) One face of *Chlamydia trachomatis*: The infectious elementary body. *Curr Top Microbiol Immunol*, 10.1007/82_2016_12.
8. Swanson AF, Ezekowitz RAB, Lee A, Kuo CC (1998) Human mannose-binding protein inhibits infection of HeLa cells by *Chlamydia trachomatis*. *Infect Immun* 66:1607–1612.
9. Taraktchoglou M, Pacey AA, Turnbull JE, Eley A (2001) Infectivity of *Chlamydia trachomatis* serovar LGV but not E is dependent on host cell heparan sulfate. *Infect Immun* 69:968–976.
10. Menozzi FD, et al. (2002) Enhanced bacterial virulence through exploitation of host glycosaminoglycans. *Mol Microbiol* 43:1379–1386.
11. Tiwari V, Maus E, Sigar IM, Ramsey KH, Shukla D (2012) Role of heparan sulfate in sexually transmitted infections. *Glycobiology* 22:1402–1412.
12. Fadel S, Eley A (2008) Differential glycosaminoglycan binding of *Chlamydia trachomatis* OmcB protein from serovars E and LGV. *J Med Microbiol* 57:1058–1061.
13. Beswick EJ, Travelstead A, Cooper MD (2003) Comparative studies of glycosaminoglycan involvement in *Chlamydia pneumoniae* and *C. trachomatis* invasion of host cells. *J Infect Dis* 187:1291–1300.
14. Stallmann S, Hegemann JH (2016) The *Chlamydia trachomatis* Ctad1 invasin exploits the human integrin β1 receptor for host cell entry. *Cell Microbiol* 18:761–775.
15. Subbarayal P, et al. (2015) EphrinA2 receptor (EphA2) is an invasion and intracellular signaling receptor for *Chlamydia trachomatis*. *PLoS Pathog* 11:e1004846.
16. Elwell CA, Ceesay A, Kim JH, Kalman D, Engel JN (2008) RNA interference screen identifies Abl kinase and PDGFR signaling in *Chlamydia trachomatis* entry. *PLoS Pathog* 4:e1000021.
17. Kim JH, Jiang S, Elwell CA, Engel JN (2011) *Chlamydia trachomatis* co-opts the FGF2 signaling pathway to enhance infection. *PLoS Pathog* 7:e1002285.
18. Méndez-Huergo SP, Blidner AG, Rabinovich GA (2017) Galectins: Emerging regulatory checkpoints linking tumor immunity and angiogenesis. *Curr Opin Immunol* 45:8–15.
19. Cerliani JP, Blidner AG, Toscano MA, Croci DO, Rabinovich GA (2017) Translating the 'sugar code' into immune and vascular signaling programs. *Trends Biochem Sci* 42: 255–273.
20. Sato S, St-Pierre C, Bhaumik P, Nieminen J (2009) Galectins in innate immunity: Dual functions of host soluble β-galactoside-binding lectins as damage-associated molecular patterns (DAMPs) and as receptors for pathogen-associated molecular patterns (PAMPs). *Immunol Rev* 230:172–187.
21. Vasta GR (2009) Roles of galectins in infection. *Nat Rev Microbiol* 7:424–438.
22. Baum LG, Garner OB, Schaefer K, Lee B (2014) Microbe-host interactions are positively and negatively regulated by galectin-glycan interactions. *Front Immunol* 5:284.
23. Chen HY, Weng IC, Hong MH, Liu FT (2014) Galectins as bacterial sensors in the host innate response. *Curr Opin Microbiol* 17:75–81.
24. Thurston TL, Wandel MP, von Muhlinen N, Foeglein A, Randow F (2012) Galectin 8 targets damaged vesicles for autophagy to defend cells against bacterial invasion. *Nature* 482:414–418.
25. Poncini CV, et al. (2015) *Trypanosoma cruzi* infection imparts a regulatory program in dendritic cells and T cells via galectin-1-dependent mechanisms. *J Immunol* 195: 3311–3324.
26. Okumura CYM, Baum LG, Johnson PJ (2008) Galectin-1 on cervical epithelial cells is a receptor for the sexually transmitted human parasite *Trichomonas vaginalis*. *Cell Microbiol* 10:2078–2090.
27. Pineda MA, Corvo L, Soto M, Fresno M, Bonay P (2015) Interactions of human galectins with Trypanosoma cruzi: Binding profile correlate with genetic clustering of lineages. *Glycobiology* 25:197–210.
28. Benatar AF, et al. (2015) Galectin-1 prevents infection and damage induced by *Trypanosoma cruzi* on cardiac cells. *PLoS Negl Trop Dis* 9:e0004148.
29. Gauthier S, et al. (2008) Induction of galectin-1 expression by HTLV-I Tax and its impact on HTLV-I infectivity. *Retrovirology* 5:105.
30. St-Pierre C, et al. (2011) Host-soluble galectin-1 promotes HIV-1 replication through a direct interaction with glycans of viral gp120 and host CD4. *J Virol* 85:11742–11751.
31. Yang M-L, et al. (2011) Galectin-1 binds to influenza virus and ameliorates influenza virus pathogenesis. *J Virol* 85:10010–10020.
32. Toledo KA, et al. (2014) Galectin-1 exerts inhibitory effects during DENV-1 infection. *PLoS One* 9:e112474.
33. Garner OB, et al. (2015) Timing of galectin-1 exposure differentially modulates Nipah virus entry and syncytium formation in endothelial cells. *J Virol* 89:2520–2529.
34. Lee PH, et al. (2015) Enterovirus 71 virion-associated galectin-1 facilitates viral replication and stability. *PLoS One* 10:e0116278.
35. Ouyang J, et al. (2011) Viral induction and targeted inhibition of galectin-1 in EBV+ posttransplant lymphoproliferative disorders. *Blood* 117:4315–4322.
36. Nita-Lazar M, Banerjee A, Feng C, Vasta GR (2015) Galectins regulate the inflammatory response in airway epithelial cells exposed to microbial neuraminidase by modulating the expression of SOCS1 and RIG1. *Mol Immunol* 68:194–202.
37. Davicino RC, et al. (2017) Galectin-1-driven tolerogenic programs aggravate *Yersinia enterocolitica* infection by repressing antibacterial immunity. *J Immunol* 199:1382–1392.
38. Suryawanshi A, Cao Z, Thitiprasert T, Zaidi TS, Panjwani N (2013) Galectin-1-mediated suppression of *Pseudomonas aeruginosa*-induced corneal immunopathology. *J Immunol* 190:6397–6409.
39. Marcos NT, et al. (2008) *Helicobacter pylori* induces beta3GnT5 in human gastric cell lines, modulating expression of the SabA ligand sialyl-Lewis x. *J Clin Invest* 118: 2325–2336.
40. Kuo C, Takahashi N, Swanson AF, Ozeki Y, Hakomori S (1996) An N-linked high-mannose type oligosaccharide, expressed at the major outer membrane protein of *Chlamydia trachomatis*, mediates attachment and infectivity of the microorganism to HeLa cells. *J Clin Invest* 98:2813–2818.
41. Fujitani N, et al. (2013) Total cellular glycomics allows characterizing cells and streamlining the discovery process for cellular biomarkers. *Proc Natl Acad Sci USA* 110: 2105–2110.
42. Horvat T, et al. (2013) Reversibility of membrane N-glycome of HeLa cells upon treatment with epigenetic inhibitors. *PLoS One* 8:e54672.
43. Cho M, Cummings RD (1996) Characterization of monomeric forms of galectin-1 generated by site-directed mutagenesis. *Biochemistry* 35:13081–13088.
44. Croci DO, et al. (2014) Glycosylation-dependent lectin-receptor interactions preserve angiogenesis in anti-VEGF refractory tumors. *Cell* 156:744–758.
45. Hatch NE, Hudson M, Seto ML, Cunningham ML, Bothwell M (2006) Intracellular retention, degradation, and signaling of glycosylation-deficient FGFR2 and craniosynostosis syndrome-associated FGFR2C278F. *J Biol Chem* 281:27292–27305.
46. Citores L, Bai L, Sørensen V, Olsnes S (2007) Fibroblast growth factor receptor-induced phosphorylation of STAT1 at the Golgi apparatus without translocation to the nucleus. *J Cell Physiol* 212:148–156.
47. Chen P-H, Chen X, He X (2013) Platelet-derived growth factors and their receptors: Structural and functional perspectives. *Biochim Biophys Acta* 1834:2176–2186.
48. Bellis SL (2004) Variant glycosylation: An underappreciated regulatory mechanism for β1 integrins. *Biochim Biophys Acta* 1663:52–60.
49. Stowell SR, et al. (2014) Microbial glycan microarrays define key features of host-microbial interactions. *Nat Chem Biol* 10:470–476.
50. Siridewa K, Fröman G, Hammar L, Mårdh P-A-A (1993) Characterization of glycoproteins from *Chlamydia trachomatis* using lectins. *APMIS* 101:851–857.
51. Kuo CC, Lee A, Campbell LA (2004) Cleavage of the N-linked oligosaccharide from the surfaces of *Chlamydia* species affects attachment and infectivity of the organisms in human epithelial and endothelial cells. *Infect Immun* 72:6699–6701.
52. Van Breedam W, Pöhlmann S, Favoreel HW, de Groot RJ, Nauwynck HJ (2014) Bittersweet symphony: Glycan-lectin interactions in virus biology. *FEMS Microbiol Rev* 38: 598–632.
53. Zúñiga E, Gruppi A, Hirabayashi J, Kasai KI, Rabinovich GA (2001) Regulated expression and effect of galectin-1 on *Trypanosoma cruzi*-infected macrophages: Modulation of microbicidal activity and survival. *Infect Immun* 69:6804–6812.
54. Stowell SR, et al. (2010) Innate immune lectins kill bacteria expressing blood group antigen. *Nat Med* 16:295–301.
55. Cagnoni AJ, Pérez Sáez JM, Rabinovich GA, Mariño KV (2016) Turning-off signaling by siglecs, selectins, and galectins: Chemical inhibition of glycan-dependent interactions in cancer. *Front Oncol* 6:109.
56. Rabinovich G, Castagna L, Landa C, Riera CM, Sotomayor C (1996) Regulated expression of a 16-kd galectin-like protein in activated rat macrophages. *J Leukoc Biol* 59:363–370.
57. Barrionuevo P, et al. (2007) A novel function for galectin-1 at the crossroad of innate and adaptive immunity: Galectin-1 regulates monocyte/macrophage physiology through a nonapoptotic ERK-dependent pathway. *J Immunol* 178:436–445.
58. Agaisse H, Derré I (2013) A *C. trachomatis* cloning vector and the generation of *C. trachomatis* strains expressing fluorescent proteins under the control of a *C. trachomatis* promoter. *PLoS One* 8:e57090.
59. Croci DO, et al. (2012) Disrupting galectin-1 interactions with N-glycans suppresses hypoxia-driven angiogenesis and tumorigenesis in Kaposi's sarcoma. *J Exp Med* 209: 1985–2000.